Environmental considerations in the AASHTO mechanistic-empirical pavement design guide: impacts on performance

Maadani, Omran; El Halim, A.O. Abd

Publisher's version / Version de l'éditeur:
https://doi.org/10.1061/(ASCE)CR.1943-5495.0000126
Journal of cold regions engineering, 31, 3, 2017-03-03

ENVIRONMENTAL CONSIDERATIONS IN THE AASHTO M-EPDG : IMPACTS ON PERFORMANCE

By

Omran Maadani, MSc.
Construction Portfolio, National Research Council Canada
1200 Montreal Road, M-20
Ottawa, Ontario K1A 0R6 Canada
Phone: (613) 993-3811
Fax: (613) 993-1866
Email: omran.maadani@nrc-cnrc.gc.ca

A. O. Abd El Halim, Ph.D., P.Eng., FCSCE Professor
Department of Civil and Environmental Engineering Carleton University
Ottawa, ON Canada
K1S 5B6
Tel: (613)520-2600, ext 5789
Email: a_halim@carleton.ca

ENVIRONMENTAL CONSIDERATIONS IN THE AASHTO M-EPDG : IMPACTS ON PERFORMANCE

ABSTRACT

This paper is a continuation of an earlier overview on the subject and presents the results of a sensitivity analysis that assessed the ability of the Mechanistic-Empirical Pavement Design Guide (M-EPDG) to portray the impact of temperature and moisture content on flexible pavements performance. The study used the most common asphalt concrete (HL3) and unbound materials (granular A and silty sand) used in Canada. Two binders (PG 52-34 and PG 58.28) and three moisture conditions (dry, wet and optimum) were chosen. Designs performed using level 3 of analysis for unbound materials and level 1 for asphalt concrete showed the M-EPDG is sensitive to binder performance grades as well as to climatic zones (cold vs. warm). However, the M-EPDG showed limited sensitivity to the state of unbound materials where permanent deformation showed negligible changes between wet, dry and optimum conditions.

Model simulations indicated rutting that accumulated throughout the 20-years design life for the warm region (Long Beach, California) was 50% more compared with that in the relatively cold region (New York). Using different soil conditions for unbound materials showed that the increase in resilient modulus from wet to dry conditions increases the total rutting by 27%. Results also demonstrated good sensitivity to the type of asphalt binder and agreed with binder type objective, where HL3 mix with the PG 58-28 binder decreased substantially the rutting by about 271 % compared with the mix prepared with the PG 52-34 binder.

INTRODUCTION

Construction of pavements in cold regions (including northern states in USA and Canada provinces, as well as countries bordering the arctic regions above the 66 latitude) require special attention due to repeated cycling of atmospheric temperature from freezing to thawing. In view of the substantial cost needed for their maintenance and rehabilitation, roads are expected to perform over long periods of use, without major distresses over a wide range of temperatures and

moistures. Nonetheless, it is not uncommon to see road failures after only three to five years of service. Thus, it is necessary to understand the effect of climatic changes on roads in the short, medium and long term with a view of incorporating improvements that help to mitigate premature failures. One such improvement may be to link the pavement structure response, influenced by environmental, operating and service requirements, as well as traffic loading, to performance quantified according to specific criteria.

Currently, pavement analysis, including that of the Mechanistic-Empirical Pavement Design Guide (M-EPDG), is based primarily on multilayered linear elastic analysis. Mechanistic characterization techniques of road materials represent one of the major improvements introduced in the M-EPDG model.

Temperature impact

Pavement modelling and design depend heavily on the temperature used to specify the performance grades for asphalt binders, load limits during spring season, and frost-free base thickness.

Mechanical properties of asphalt materials, such as the elastic modulus, are often measured at room temperature (AASHTO design guide, 1993). However, an asphalt concrete mat may experience a wide range of thermal regimes during the different climatic seasons. It is well known that asphalt concretes become brittle subjected to temperatures lower than – 5^{o}C (Wright and Zheng, 1994). On the other hand, high temperatures cause flow and fluidity of asphalt cements which make asphalt concretes soft and prone to large permanent deformations in the form of rutting when subjected to stresses induced by applied traffic loads. These plastic deformations are mainly related to temperature and the number of loading applications (Wright and Zheng, 1994).

The modulus of elasticity “E” has been used to characterize pavement structures. This approach assumes that asphalt concretes exhibit a linear elastic response. However, most of the asphalt mixes used in pavement structures are nonlinear. Uzan, 1996; Perl *et al* ., 1983; Sides *et al.*, 1985; Kim *et al.*,1997; Wright and Zheng, 1994 and Lu and Wright, 1998, have shown that the asphalt

concrete behavior has four distinct responses; elastic, viscoelastic, visco-plastic and plastic behavior depending on loading and temperature. However, Di Benedetto and De La Roche, 1998 considered the behavior of asphalt concrete as complex visco-elasto-plastic, which can be considered purely elastic and viscoelastic at low strain amplitudes. At low temperatures, the asphalt concrete behavior is a combination of elastic and slight linear viscoelastic.

The dynamic modulus is the stiffness component of the complex modulus that has been implemented in the M-EPDG. The American Association of State Highway and Transportation Officials provisional test standard (AASHTO TP62, 2003) is a stress-controlled version of the complex modulus test and focuses on capturing the visco-elastic response of asphalt concrete (AC) materials. Traffic loading is simulated in the laboratory with a haver-sine cyclic load applied to the specimen and adjusted so that the specimen is subjected to an axial strain between 50 and 150 micro-strains (με). The response of the material exhibits a phase lag, (Fig. 1). The M-EPDG structural response model is based on conducting linear elastic analysis and hence, the phase angle is not being considered in the analysis. Incorporation of the impact of the viscous response in conducting structural analysis will be considered in future design.

The laboratory test may be conducted under a stress or strain controlled mode. In the stress-controlled mode, the stress applied is given by:

$$\sigma = \sigma_0 \mathrm{Sin}\,(\omega.t) \tag{1}$$

And the corresponding strain is given by:

$$\varepsilon = \varepsilon_0 \mathrm{Sin}\,(\omega.t-\phi) \tag{2}$$

In the strain-controlled mode, the applied strain is expressed as:

$$\varepsilon = \varepsilon_0 \mathrm{Sin}\,(\omega.t) \tag{3}$$

And the corresponding stress is given by:

$$\sigma = \sigma_0 \mathrm{Sin}\,(\omega.t+\phi) \tag{4}$$

Where σ_0 is the stress amplitude, ε_0 is the strain amplitude (see Fig. 1) and ω is the angular velocity related to the frequency *f* by Equation 5:

$$\omega = 2\pi f \tag{5}$$

Angle ∅ is the phase lag between the strain and the stress signal (see Fig. 1). The phase angle is an indicator of the degree of the visco-elastic behavior of an asphalt concrete mix. The ∅ ranges from 0 to π/2. A value of 0 is an indicator of purely elastic behavior, while a value of π/2 is an indicator of purely viscous behavior. The phase lag ∅ between signals associated with the applied stress ($\emptyset_1$) and the corresponding strain ($\emptyset_2$), it should be calculated as the difference between them in radians. The phase lag in radians is then converted into phase angle in degrees according to Equation 6:

$$\emptyset = (\emptyset_1 - \emptyset_2) \times \frac{180}{\pi} \tag{6}$$

Regardless of the test mode used, the ratio of the stress to strain amplitudes defines the absolute value of the complex modulus known as the dynamic modulus and is expressed by Equation 7:

$$|E^*| = \frac{\sigma_o}{\varepsilon_o} \tag{7}$$

In the new design guide, creep compliance and tensile strength tests are considered the most promising for predicting the low-temperature performance of asphalt concrete mixtures. At lower loading rates and high temperatures, the behavior is nonlinear viscoelastic, visco-plastic and plastic. Viscoelastic theory to model asphalt concrete was applied by Schapery and Park, 1999 using uniaxial monotonic loading and by Lee, 1996; Kim and Daniel, 1997 and Lee and Kim, 1998 using cyclic loading.

Moisture impact

The resilient modulus parameter (M_R) was adopted for the characterization of unbound materials in the AASHTO design guide (NCHRP, 2004). The resilient modulus along with the Poisson's ratio is used in the pavement response model to quantify the stress dependent stiffness of unbound material layers.

Each time a load passes over a pavement structure, the pavement rebounds less than its deflection under the load. After repeated loading sequences, each layer accumulates only a small amount of permanent deformation, which is recoverable with time. This is called resilient deformation and it can be defined as the ratio of the applied deviator stress, (σ_d) to the recoverable resilient strain (ε_r) (Equation 8):

$$M_R = \frac{\sigma_d}{\varepsilon_r} \quad (8)$$

Where;

M_R= resilient modulus; σ_d = repeated deviator stress (σ_1- σ_3); ε_r = recoverable axial strain in the direction of principal stress; σ_1= total axial stress (Major principle stress); σ_2, σ_3 = applied confined pressure (minor stress); and $\sigma_2 = \sigma_3$.

This study presents a sensitivity analysis examining the ability of the model to account for the impact of seasonal variations, specifically temperature and moisture content. It considered

- the most common asphalt concrete and unbound materials used in Canada: HL3 mix and granular material A and silty sand
- two binder types: PG 52-34 and PG 58-28
- three levels of moisture conditions: dry, wet and optimum
- level 3 of analysis for unbound materials since there was no access to level 1 which involves finite element analysis
- level 1 analysis for asphalt concrete materials
- warm and relatively cold areas.

EXPERIMENTAL WORK

Asphalt concrete

The complex modulus, creep compliance, indirect tensile strength, binder shear complex modulus and phase angle are the primary input for level 1 of analysis required by the AASHTO design guide (NCHRP, 2004) for Hot Mix Asphalt (HMA).

Sample preparation

The Super-Pave for 12.5 mm nominal maximum size (SP 12.5) mix was used in this study. Design aggregate structure is selected using control points and a restricted zone on the 0.45 power gradation. Job mix formula was used with different materials gradation to make the super-pave blends of aggregate developed as part of the HMA mix design process and used in the production of HMA that satisfies the requirements of Ontario Provincial Standard Specification, OPSS 1003 (2002) for fine and coarse limits as shown in Fig. 2.

Samples of the SP 12.5 mix, using performance grade using performance grades PG 52-34 and PG 58-28, were prepared at National Research Council of Canada following the requirements of the AASHTO design guide (NCHRP, 2004) as detailed in the sequences below:

1. The SuperPave mixes were designed according to LS 309 (Ministry of Transportation Ontario 2001);
2. Mixtures were compacted using a gyratory compactor. The number of gyrations was controlled to produce samples with 100 mm in height and radius, as specified by AASHTO TP62 (2003), and various air voids content;
3. The Physical properties such as bulk specific gravity, maximum specific gravity and air voids content were determined according to AASHTO T166 (2010), T209 (2010) and T269 (1997), respectively;

4. The determined binder content was used to prepare samples for the complex modulus test; and
5. Aggregate binder mixture were prepared using mechanical mixer and aged in an oven for two hours at the binder's compaction temperature as per the requirements of AASHTO PP2 (2000).

It should be noted that although many agencies may follow the AASHTO grading requirements, some agencies may use different specifications. In most cases, there may be minor modifications to the AASHTO requirements.

Table 1 shows the summary of the SP 12.5 mixes physical properties for PG 52-34 and PG 58-28 binders.

Dynamic modulus

Strain-controlled test were used in this study. A sinusoidal axial deformation (tension and compression) corresponding to 120 micro-strain was applied at a given temperature and loading frequency. The resulting axial stress was measured and used together with the applied strain to calculate the dynamic modulus (E*). The test series consisted of five test temperatures (-12, 5, 20, 38, and 54° C) and six loading frequencies (0.1, 0.3, 1.0, 5, 10, and 20 Hz.) Each specimen was tested for the 30 combinations of temperature and frequency starting with the lowest temperature and proceeding to the highest. Testing at a given temperature began with the highest frequency of loading and proceeded to the lowest. Tables 2 and 3 show the results of calculated dynamic modulus for SP 12.5 mix using PG52-34 and PG 58-28 binders, respectively.

The dynamic modulus of the asphalt concretes for the two binders are plotted in Fig. 3 at a frequency of 20 Hz. As expected, the asphalt concrete using the binder PG 58-28 is stiffer than

that prepared using the binder PG 52-34. This confirms the intended use of PG 58-28 to minimize rutting and PG 52-34 to minimize thermal cracking.

Creep compliance and tensile strength

The creep compliance ($D_{(t)}$) and tensile strength (σ_t)were determined following the requirements of AASHTO T322 (2003). The creep compliance was determined by applying a static compressive load of fixed magnitude along the diametric axis of a specimen for duration of 100 seconds. The measured horizontal and vertical deformations from each side and axial load were used to calculate the creep compliance using the series of Equations 9 to 13 (AASHTO T322 (2003).

$$C_{CMPL} = 0.6354\left(\frac{X}{Y}\right)^{-1} - 0.332 \quad (9)$$

$$0.20 \leq \frac{t}{D} \leq 0.65 \quad (10)$$

$$v = -0.1 + 1.480\left(\frac{X}{Y}\right)^{2} - 0.778\left(\frac{t}{D}\right)^{2}\left(\frac{X}{Y}\right)^{2} \quad (11)$$

$$0.05 \leq v \leq 0.50 \quad (12)$$

$$D_{(t)} = \frac{\Delta X_{(t)} \times D \times t}{P \times GL} \times C_{CMPL} \quad (13)$$

Where;

$D_{(t)} = \text{Creep Compliance}, MPa^{-1}$; X= Horizontal deformation, mm; Y= Vertical deformation, mm; t = Thickness of specimen, mm; D= Diameter of specimen, mm; P = Constant load, N; GL = Gauge length, mm

The average creep compliance of each test series consisted of three test temperatures (-20, -10 and 0^{o} C) which are needed as input into the software to calculate low temperature cracking. Tables 4 and 5 show the measured results of creep compliance of the SP 12.5 mix for PG 52-34 and PG 58-28 binders, respectively. The results are plotted in Fig. 4 which shows that the asphalt concrete prepared using the binder PG 58-28 is stiffer compared to the one prepared using the binder PG 52-34. This suggests that the asphalt concrete prepared using the binder PG 52-34 is more suitable for minimizing cracking due to low temperature.

The indirect tensile strength was measured by applying load on the HMA specimen along its diametric axis at constant rate of 12.5 mm/minute until failure. The test was performed at a temperature of -10^{o} C. The indirect tensile strength (σ_t) was calculated using Equation 14.

$$\sigma_t = \frac{2P_f}{\pi \times t \times D} \tag{14}$$

Where;

$\sigma_t = \text{Tensile strength, MPa}$; P_f = Tensile strength at failure, N; t = specimen thickness, mm; D = specimen diameter, mm

The determined tensile strength was 2.66 and 3.73 MPa for the asphalt concrete prepared using the PG 52-34 and PG 58-28 binders, respectively.

Asphalt binder

In this study, the complex modulus and phase angle of the asphalt binders (PG 52-34 and PG 58-28) were calculated using the measured dynamic modulus for the SP 12.5 mix. Equation 15 was used to determine the binder complex modulus (G^*) at different temperatures and a loading rate of 1.59 Hz (10 rad/sec).

$$G^* = \frac{E^*}{2(1+V)} \quad (15)$$

Where;

G^* = binder complex shear modulus, Pa; E^*= dynamic modulus; v = poisons' ratio

Equations 16 and 17 were used to determine the binder viscosity and phase angle, respectively.

$$loglog(\eta) = A = VTS \log TR \quad (16)$$

Where

H = viscosity, cp; T = temperature, Rankin; A = 10.035 (Regression intercept); VTS = -3.35 (regression slope of viscosity temperature)

$$\eta = \frac{G^*}{10}\left(\frac{1}{sin\delta}\right)^{-4.8628} \quad (17)$$

Where;

δ = binder phase angle

The determined binder complex modulus and phase angle for the SP 12.5 mixes using the PG 58-28 and PG 52-34 binders are shown in given in Table 6.

Table 6: Binder complex modulus and phase angle

PG Binder	52-34		58-28	
T, °C	G* , MPa	δ, Degree	G* , MPa	δ, Degree
-12	3676	76	8054	77
5	2090	75	5220	76
20	505	73	2213	76
38	110	71	370	73
54	50	69	126	71

Unbound and sub-grade materials

The NCHRP, 2004 Design Guide has adopted the Resilient Modulus to characterize the mechanistic response of the unbound and sub-grade materials. The advanced design level recommends using actual laboratory test data of the resilient modulus determined under simulated measured environmental parameters and traffic loading conditions.

The resilient modulus, moisture content, soil density, Atterberg parameters, and sieve analysis are the primary parameters needed for level 3 of analysis.

Sieve analysis and Atterberg limits

The gradation analysis for all materials used in this study was conducted according to AASHTO T88 (1997) and is given in Table 7. The liquid and plastic limit of these materials were determined using ASTM standard test D4318 (2005) and are shown in Table 8.

Density

AASHTO T99(1997) was used to determine the relation between the moisture content and density of soils compacted in a mold of a 101.6 or 152.4 mm diameter mold with a 2.5 kg rammer dropped from a height of 305 mm. The results are shown in Table 9.

Table 9 shows that a 2% and 7.5% decrease from optimum moisture content (dry of optimum) leads to a decrease of 2.5% and 7.5 % in the dry density for the granular and silty sand materials, respectively. The results in Table 9 indicates that of moisture content was above the optimum (wet of optimum) by a 1% and 3 % increase which leads to decrease of 5% and 14 % in the dry density for the granular and silty sand materials, respectively. These findings clearly indicate and confirm that deviations from optimum conditions lead to a reduction in the dry density. This deviation is more significant for wet of optimum conditions.

Resilient modulus

The resilient modulus was determined using the AASHTO 307 (2003) procedure for representative material samples (granular material A and silty sand). The resilient modulus (M_R) was measured for a number of load applications following the sequences shown in the testing

procedure. Each cycle has two load segments; first segment lasts for 0.1 seconds and the second segment and lasts for 0.90 seconds of sine loading period. Fig. 5 shows a maximum deviator load being applied for duration of .05 seconds throughout the segment number one. Then, the load is released for another 0.05 seconds. The rest of the cycle is represented by duration of 0.9 seconds. The average of the last few points of the last segment is taken to calculate the resilient modulus. The results are given in Table 9.

Impact of Moisture content on the Resilient Modulus

The resilient moduli given in Table 9 show that at lower moisture contents the resilient modulus tends to increase, whereas at higher moisture contents the resilient modulus decreases. Decreasing the water content below the optimum moisture content by 2% increases the resilient modulus by15%. However, increasing the water content above the optimum moisture content with 1 % decreases the resilient modulus by11 %.

SENSITIVITY ANALYSIS

A number of runs were performed to examine the ability of the AASHTO design guide (NCHRP, 2004) software and the incorporated Enhanced Integrated Climatic Model (EICM) to capture the impact of seasonal variations and their ability to simulate changes, in the behavior and characteristics of pavement and unbound materials that concur with climatic conditions over the design period.

Due to the limitation in the thickness of road layers that can be used in the new design guide, this study considered a variation of the in-situ conditions. Fig. 6 shows the difference between the actual road structure materials layer thickness and the maximum allowable thickness of road layers imposed by the new design guide software. The results of the experimental work were used as input into the new design guide to perform a number of runs covering a number of parameters. The details of the runs are shown in Table 10.

Input data

The AASHTO design guide (NCHRP, 2004) provides 3 levels of input depending on the importance of the project and the availability of the project design inputs. Following the recommendation of the design guide, laboratory work was performed as explained in previous sections and the results were used as input for level 1 for asphalt concrete and level 3 for unbound materials. Details of traffic data used are shown in Table 11. The climate database incorporated in the new design guide does not include the city of Ottawa, but due to the similarity in weather the city of Chicago was selected.

Effect of M-EPDG layer thickness limitation on permanent deformation

As previously mentioned, the AASHTO design guide (NCHRP, 2004) software includes an upper limit thickness of 940 mm for the base layer and 1300 mm for the sub-base layer. This forced dividing the thick base course materials to base and sub-grade materials as shown in Fig. 6.

This limitation of the M-EPDG warranted examining the effect of dividing an unbound layer into two layers in terms of performance. This was achieved by comparing the two sections shown in Fig. 7 where the base layer of 940 mm was divided into two sections; a 432 mm thick base layer and a 508 mm thick sub-grade composed of the same material (Granular A). The comparison focused on the optimum condition state of this material.

The total permanent deformation for both bound and unbound materials for the two sections considered is shown in Fig. 8. It is clear that dividing an unbound layer into two layers of the same material does not affect the performance.

Effect of binder type on asphalt concrete permanent deformation

Two mix types, namely PG 52-34 and PG 58-28 were used to evaluate the sensitivity of the model to different binder grades. The permanent deformation of the asphalt concrete layer using these binders for different moisture conditions of the unbound layer is shown in Fig. 9.The softer PG 52-34 binder resulted in an increase of 271% of the asphalt concrete rutting compared with PG 58-

28. Predicted rutting performance is in agreement with the laboratory results of dynamic modulus which indicated that PG 58-28 produced stiffer mixes than PG 52-34.

Effect of climate on asphalt concrete permanent deformation

Model runs to examine the effect of temperature on asphalt concrete rutting were carried out using two climatic files with different mean annual air temperatures (MAAT) of 20^{o} C (Long Beach, California) and 10^{o} C (New York). Rutting accumulated throughout the 20 years design life was evaluated using the optimum conditions for the unbound materials. The results are given in Fig 10. It is clear that rutting predictions for the warm region (Long Beach, California) were about 50% higher than for the relatively cold region (New York). The M-EPDG model exhibited good sensitivity to different climatic zones.

Effect of unbound material condition on permanent deformation

To investigate the ability of the M-EPDG level 3 of analysis to capture the impact of the state (dry, optimum and wet), resilient modulus and density of unbound materials, the permanent deformation of the base and sub-grade materials were examined. The results of model runs performed using both binder grades are shown in Fig 11 and 12. Regardless of the binder grade used, the permanent deformation curves of the dry, optimum and wet conditions showed little differences. In fact, at 20 years of service, the accumulated permanent deformation at these moisture conditions did not differ by more than 1.3 and 0.4 mm for the base material and the sub-grad material, respectively. These differences are within the calculation margin of errors which suggest that the level 3 of analysis is not sensitive to the unbound material conditions.

CONCLUSIONS AND RECOMMENDATION

The experimental work carried on the asphalt concrete and unbound materials showed that:

- the dynamic modulus, proposed to characterize asphalt concrete materials, differentiated between different binder performance grades.
- the asphalt concrete with the binder PG 58-28 is more suitable than the one for PG 52-34 to minimize rutting

- the asphalt concrete with the binder PG 52-34 is more suitable than the one for PG 58-28 to minimize low temperature cracking
- the resilient modulus, proposed to characterize unbound materials, is sensitive to the moisture state.

The sensitivity analysis performed showed that:

- the thickness limitations included in the M-EPDG does not affect the performance, even when a thick layer is replaced with two layers of the same material
- the model is sensitive to the binder type. The softer binder (PG 52-34) experienced a 270% increase in asphalt concrete rutting compared to the stiffer binder (PG 58-28). This confirms that the stiffer binder is more suitable to minimize rutting of asphalt concrete layers
- the model is sensitive to climatic zones. Rutting predictions for the warm region (Long Beach, California) are about 50% higher than those for the cold region (New York)
- the model has limited sensitivity to the state of unbound materials. Permanent deformation of the base and subgrade materials showed almost no difference when different states (dry, optimum and wet) were used.

This study recommends introducing nonlinear analytical methods to improve the model sensitivity, since the current model employs linear elastic analysis with permanent deformation prediction depending on empirical models.

ACKNOWLEDGMENT

The author is also grateful to the National Research Council Canada for their financial support and guidance to pursue this study. Also the author wishes to express his appreciation to Dr. Morched Zegal, National Research Council of Canada, for his suggestion, support, encouragement and guidance throughout the course of this work.

REFERNCES

1. AASHTO guide for design pavement structures 1993. American association of state highway and transportation officials, Washington, D.C.
2. AASHTO TP62, 2003. Standard method of test for determining dynamic modulus of hot-mix asphalt concrete mixtures.
3. AASHTO T166, 2010. Bulk specific gravity of bituminous paving mixtures using saturated surface dry specimens
4. AASHTO T209, 2010. Theoretical maximum specific gravity and density of bituminous paving mixture.
5. AASHTO T269, 1997. Percent air voids in compacted dense and open bituminous paving mixtures.
6. AASHTO PP2, 2000. Standard practice for mixture conditioning of hot mix asphalt.
7. AASHTO T322, 2003. Standard method of test for determining the creep compliance and strength of hot-mix asphalt using the indirect tensile test device.
8. AASHTO T88, 1997. Standard method of test for particle size analysis of soils nineteenth edition.
9. AASHTO T99, 2010. Moisture density relations of soils using a 2.5 kg rammer and a 305 mm drop.
10. AASHTO T307, 2003. Standard method of test for determining the resilient modulus of soils and aggregate materials, Washington, D.C.
11. ASTM D4318, 2005. Test methods for liquid limit, plastic limit and plasticity index of soils.
12. Di Benedetto, H. and De La Roche, C. 1998. State of the art on stiffness modulus and fatigue of bituminous mixtures. RILEM Report 17. Taylor and Francis, London, UK. Pp. 69-118.
13. Kim, J. R.; Drescher, A. and Newcomb, D. E., 1997. Rate sensitivity of asphalt concrete in triaxial compression", Journal of materials in civil engineering, v9, n2, pp 76-84.
14. Kim, Y. R. and Daniel, J. S., 1997. Development of a Mechanistic Fatigue prediction model for aging asphalt-aggregate mixtures." Final report submitted to Western Research Institute.
15. Lee, H. J., 1996. Uniaxial constitutive modelling of asphalt concrete using viscoelasticity and continuum damage theory." Ph.D. Dissertation, North Carolina State University, Raleigh, NC.
16. Lee, H. J. and Kim, Y. R., 1998. Viscoelastic constitutive model for asphalt concrete under cyclic loading." ASCE Journal of engineering Mechanics, Vol. 124, No. 11, pp. 1224-1232.

17. LS 309, 2001. Ministry of Transportation Ontario, laboratory testing manual.
18. Lu, Y. and Wright, P., 1998. Numerical approach of visco-elasoplastic analysis for asphalt mixtures" Comp. and Struct., 69(2), 139-147.
19. NCHRP. 2004. Guide for mechanistic-empirical design of new and rehabilitated pavement structures (MEPDG). Project 1-37A. Transportation Research Board, national Research Council, Washington, D.C.
20. Ontario Provincial Standard Specification, OPSS1003, 2013. Material specification for aggregate hot mix asphalt.
21. Perl, M.; Uzan, J. and Sides, A., 1983. Visco-Elasto-Plastic constitutive law for a bituminous mixture under repeated loading.", Transportation research record 911, TRB, National Research Council, Washington, D.C., pp.20-27
22. Schapery, R. A. and Park, S. W., 1999. Methods of interconversion between linear viscoelastic material functions. Part II-an approximate analytical method." International Journal of solids and structures, Vol. 36, pp.1677-1699.
23. Sides, A.; Uzan, J. and Perl, M., 1985. A comprehensive viscoelastic-plastic characterization of sand-asphalt compressive and tensile cycling loading. J. Testing and evaluation, 13(1), pp49-59
24. Uzan, J., 1996. Asphalt concrete characterization for pavement performance prediction. Journal asphalt paving technology, AAPT, Volume 65, pp573-607
25. Wright, P. and Zheng, L., 1994. ViscoElastoPlastic behavior of a hot rolled asphalt mixture under repeated loading and the effects of temperature", 4th international conference, bearing capacity of roads and airfields, Minneapolis, MN, pp 1035-1065.

Table 1: Physical properties of Mix SP 12.5

Properties	MTO Requirements	PG test results	
		52-34	58-28
Asphalt content, %	3% - 5%	4.0	4.4
VMA %	14% (MIN)	12.8	14.7
VFA %	65% - 75%	70.0	73.8
G_{mm}, % @ $N_{initial}$	90.0	89.0	89.0
G_{mm}, % @ N_{design}	98.0	96.5	96.7
Dust to Binder Ratio ($P_{0.075}$ / P_{be})	0.6 - 1.4	1.11	1.11

Table 2: Dynamic modulus results for PG 52-34

T, °C	E^*, MPa					
	Frequency, Hz					
	0.1	0.3	1	5	10	20
-12	6783	8021	9568	11979	13312	15138
5	3079	4083	5342	7384	8459	10013
20	579	842	1244	2054	2592	3422
38	121	171	263	486	656	932
54	67	96	121	212	291	412

Table 3: Dynamic modulus results for PG 58-28

T, °C	E^*, MPa					
	Frequency, Hz					
	0.1	0.3	1	5	10	20
-12	18008	19737	21496	23193	24330	24957
5	9233	11267	13612	16877	18138	19716
20	2783	4108	5617	8043	9118	10288
38	342	525	874	1723	2336	3176
54	142	183	294	600	825	1193

Table 4: Creep compliance results of the SP 12.5 mix using PG 52-34

Loading time, sec	Creep compliance (1/MPa)		
	Low at -20^{o}C	Mid at -10^{o}C	High at 0^{o}C
1	226	387	727
2	234	421	884
5	253	467	1070
10	267	517	1279
20	281	573	1528
50	303	667	1980
100	323	773	2424

Table 5: Creep compliance results of the SP 12.5 mix using PG 58-28

Loading time, sec	Creep compliance (1/MPa)		
	Low at -20^{o}C	Mid at -10^{o}C	High at 0^{o}C
1	114	125	158
2	120	137	177
5	125	147	220
10	129	158	259
20	133	166	303
50	142	176	386
100	149	190	474

Table 6: Binder complex modulus and phase angle

PG Binder	52-34		58-28	
T, ^{o}C	G* , MPa	δ, Degree	G* , MPa	δ, Degree

-12	3676	76	8054	77
5	2090	75	5220	76
20	505	73	2213	76
38	110	71	370	73
54	50	69	126	71

Table 7: Sieve analysis for granular and silty sand materials

Sieve size, mm	Passing, %	
	Granular Material A	Silty Sand
0.075	4.8	2.2
0.300	8.1	23.9
0.600	11.5	50.4
1.18	17.4	74.4
2.36	27.9	90.4
4.75	43.8	99.9
9.5	66.6	100.0
12.5	81.2	
19	95.5	
25	100.0	

Table 8: Plasticity properties for granular and silty sand materials

Soil type	Plasticity Index, PI	Liquid limit, LL
Granular material A	8.4	28.7
Silty Sand	31	45

Table 9: Physical properties for granular and silty sand materials

Classification	Material	Soil condition	M_R, MPa	Moisture content, %	Density, kN/m^3
Base	Granular material A	Dry	169	3.4	21
		Optimum	148	5.2	22
		Wet	131	5.9	21
Subgrade	Silty Sand	Dry	105	3.6	18
		Optimum	70	11.1	19
		Wet	64	13.9	17

Table 10: Details of runs

Classification	Material	Soil condition	M_R, MPa	moisture content, %	Density, kN/m^3	Maximum Code thickness, mm	Run
Base	GA	Dry	169	3.4	21	940	R1
		OPC	148	5.2	22		R2
		Wet	131	5.9	21		R3
Subgrade	GA	Dry	169	3.4	21	1300	R1
		OPC	148	5.2	22		R2
		Wet	131	5.9	21		R3
Subgrade	Silty Sand	Dry	105	3.6	18	Last	R1
		OPC	70	11.1	19		R2
		Wet	64	13.9	17		R3

Table 11: Traffic input data

Input description	Values
Design life (years)	2
Number of lanes in design direction	2
Percentage of trucks in design direction	50
Percentage of trucks in design lane	95
Operated speed, mph	45
Traffic, AADT	1000
Traffic growth, %	4

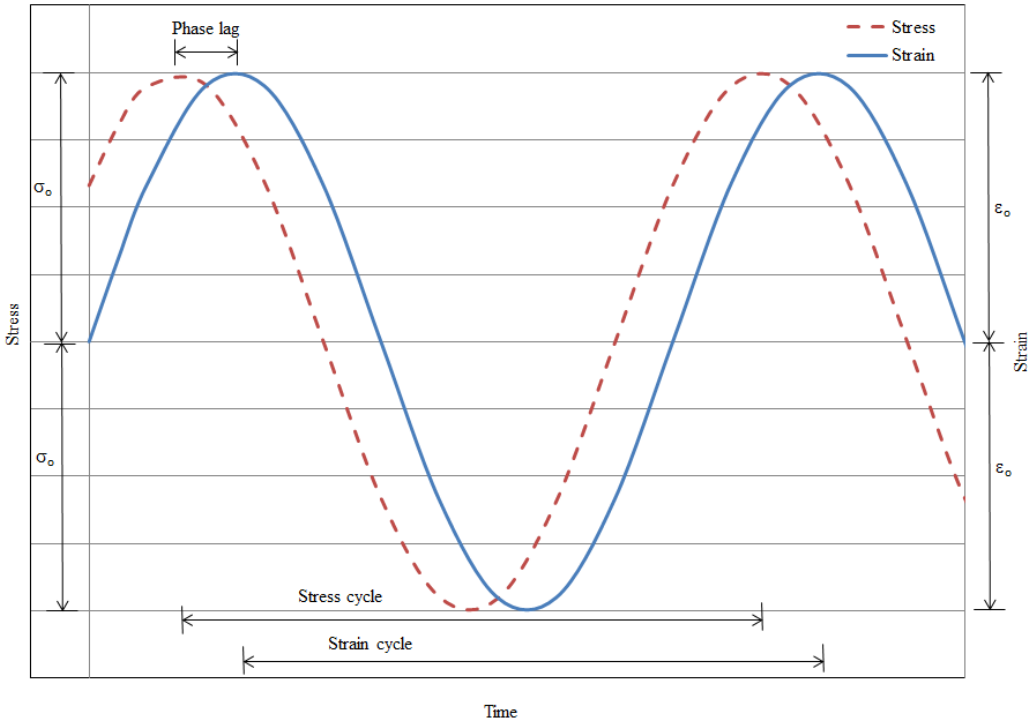

Fig 1. Typical visco-elastic response of asphalt concrete.

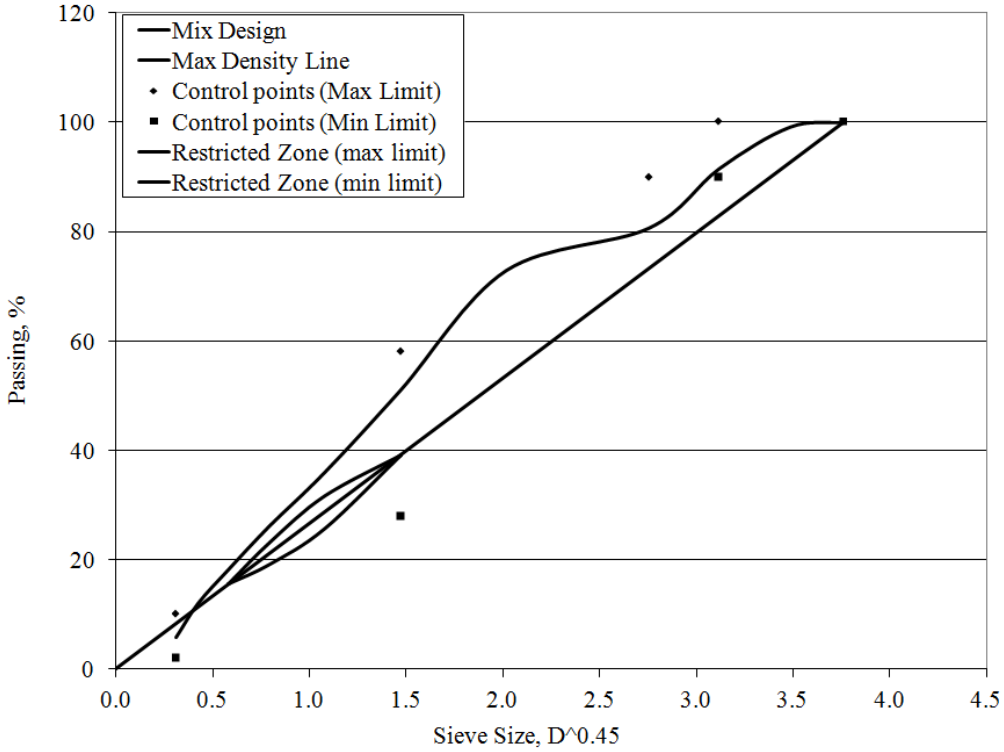

Fig 2. Aggregate grain size distribution

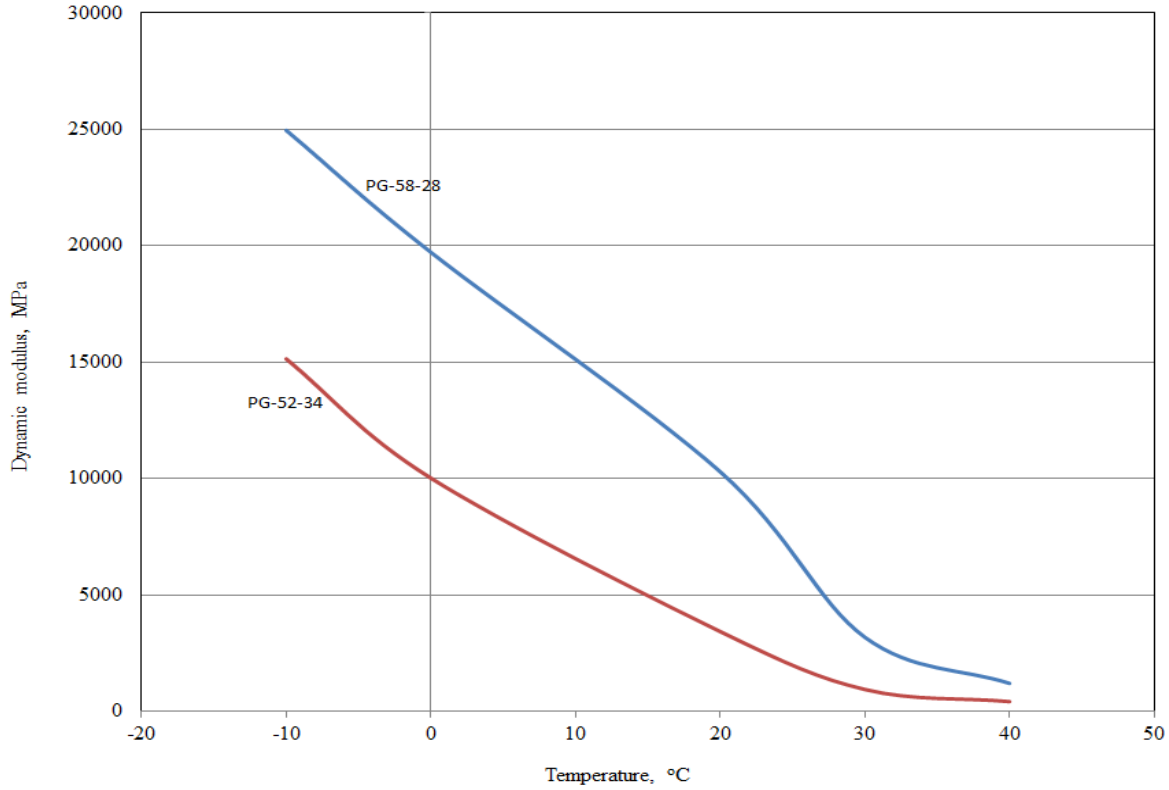

Fig 3. Dynamic modulus of HL3 asphalt concrete mixes at frequency of 20 Hz

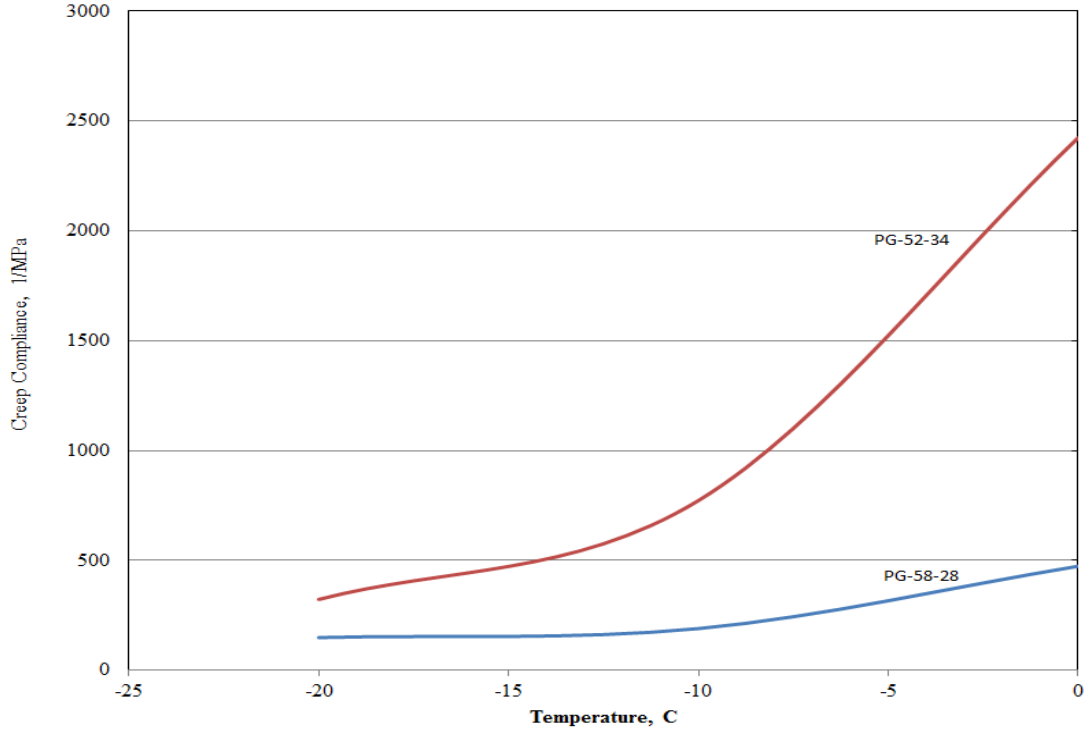

Fig 4. Creep compliance for HL3 mixes

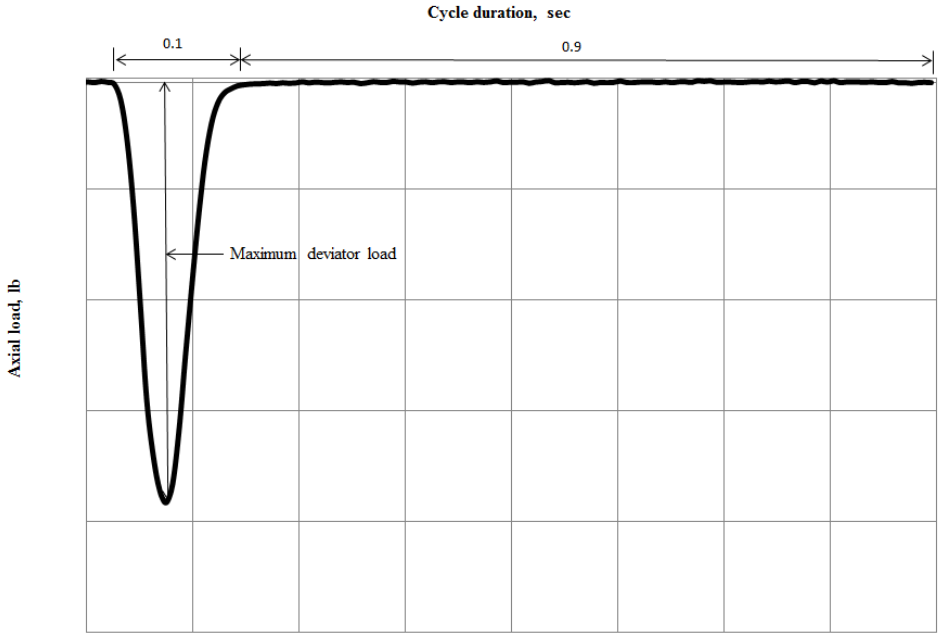

Fig 5. Axial load per cycle

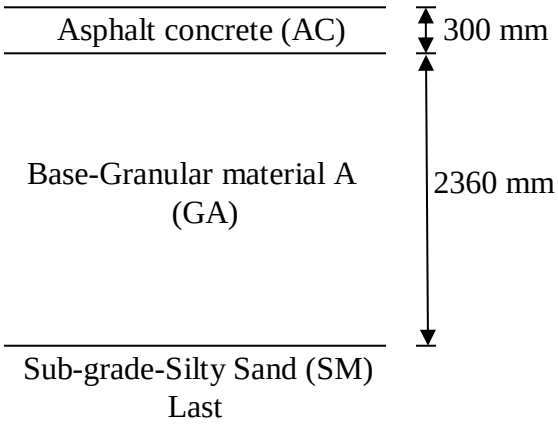

Fig 6a. Actual layers thickness

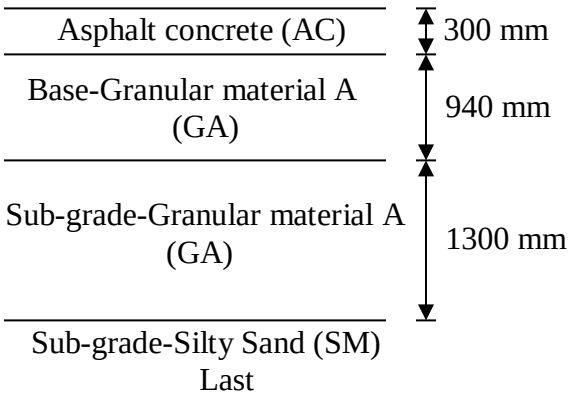

Fig 6b. Software limitation of layers thickness

Fig 6. Pavement road structure layers

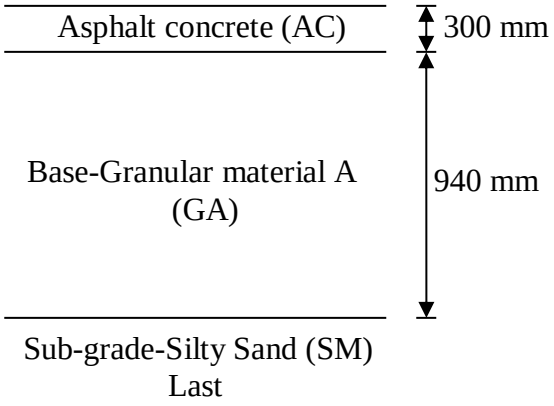

Fig 7a. Section 1

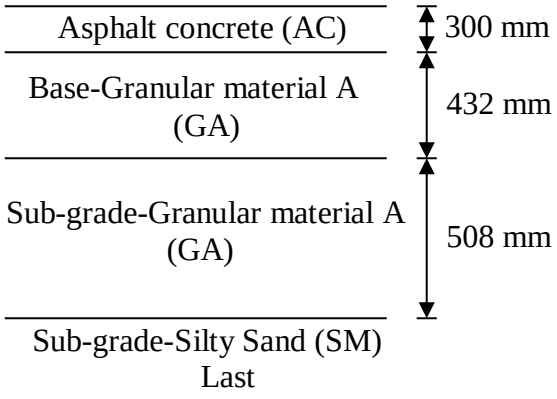

Fig 7b. Section 2

Fig 7. Sections considered investigating thickness limitation in the MEPDG

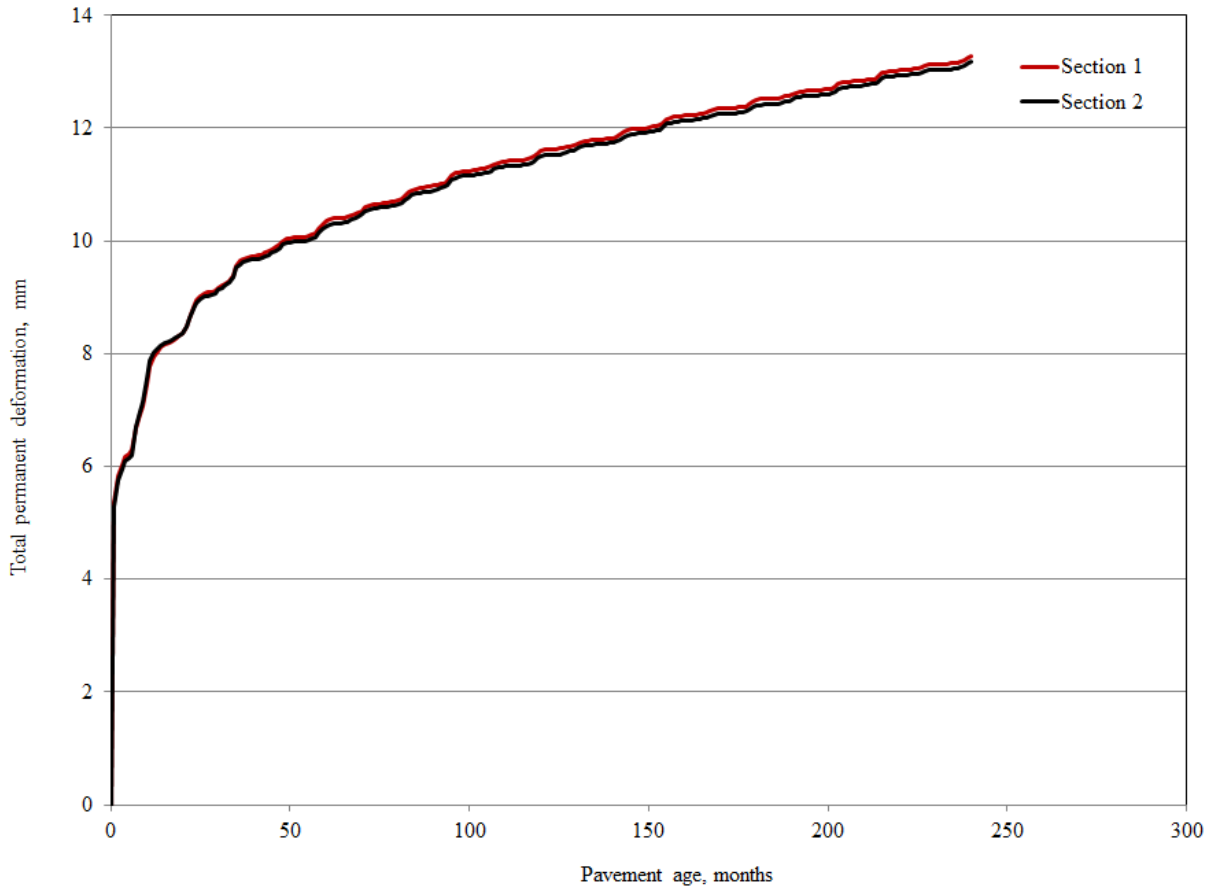

Fig 8. Effect of software upper limit on permanent deformation

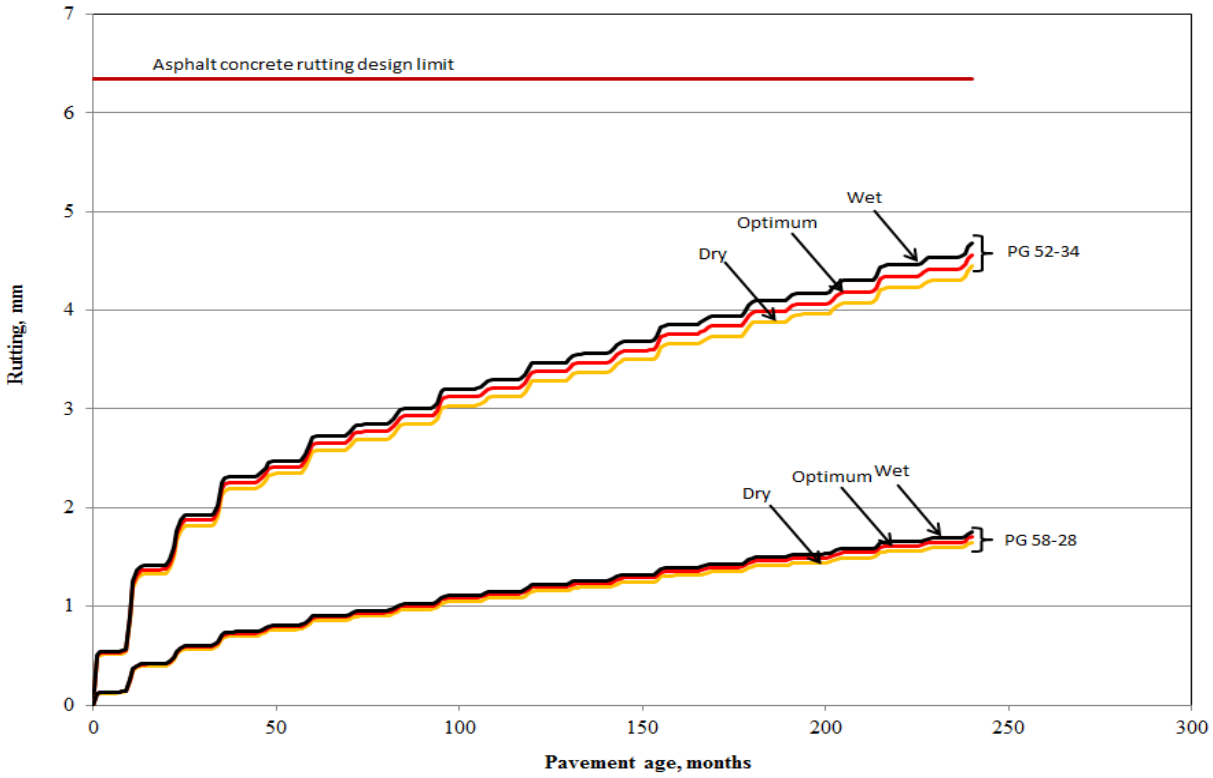

Fig 9. Permanent deformation of two HMA binders

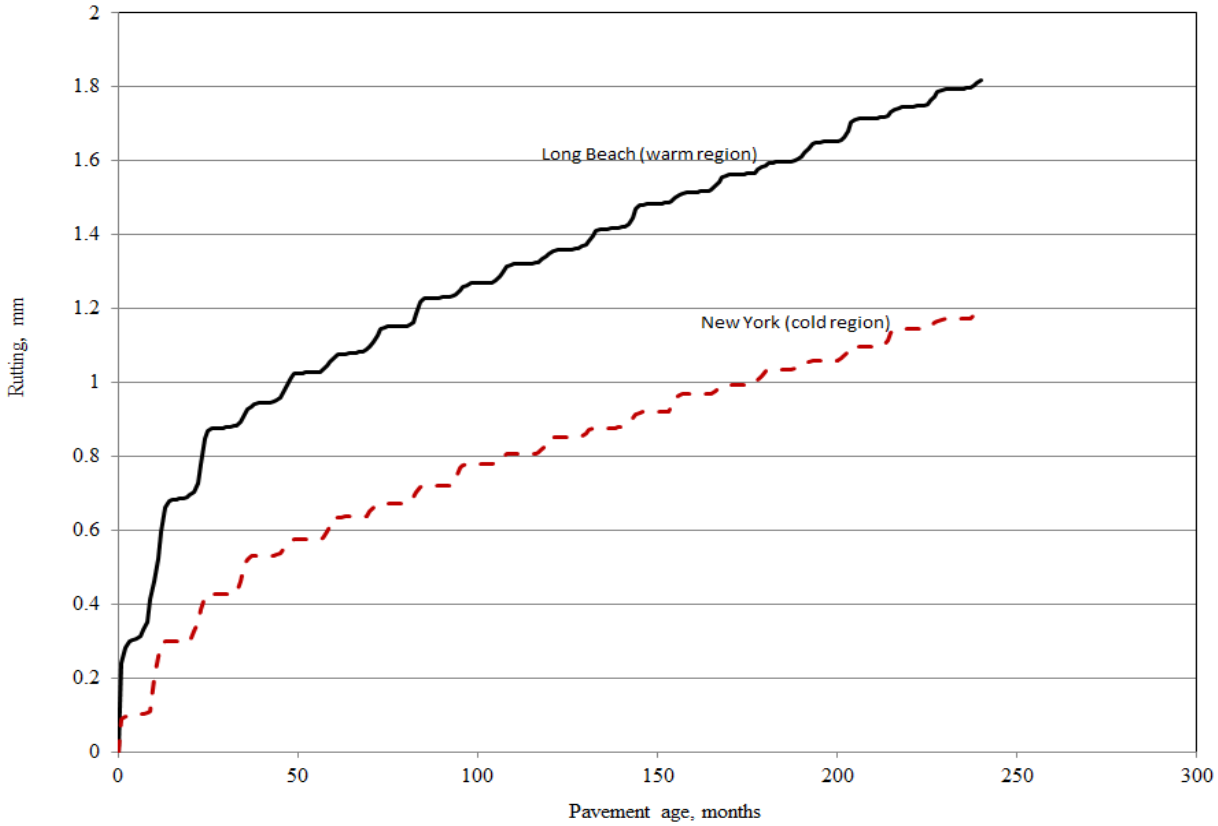

Fig 10. Effect of environment on asphalt concrete rutting

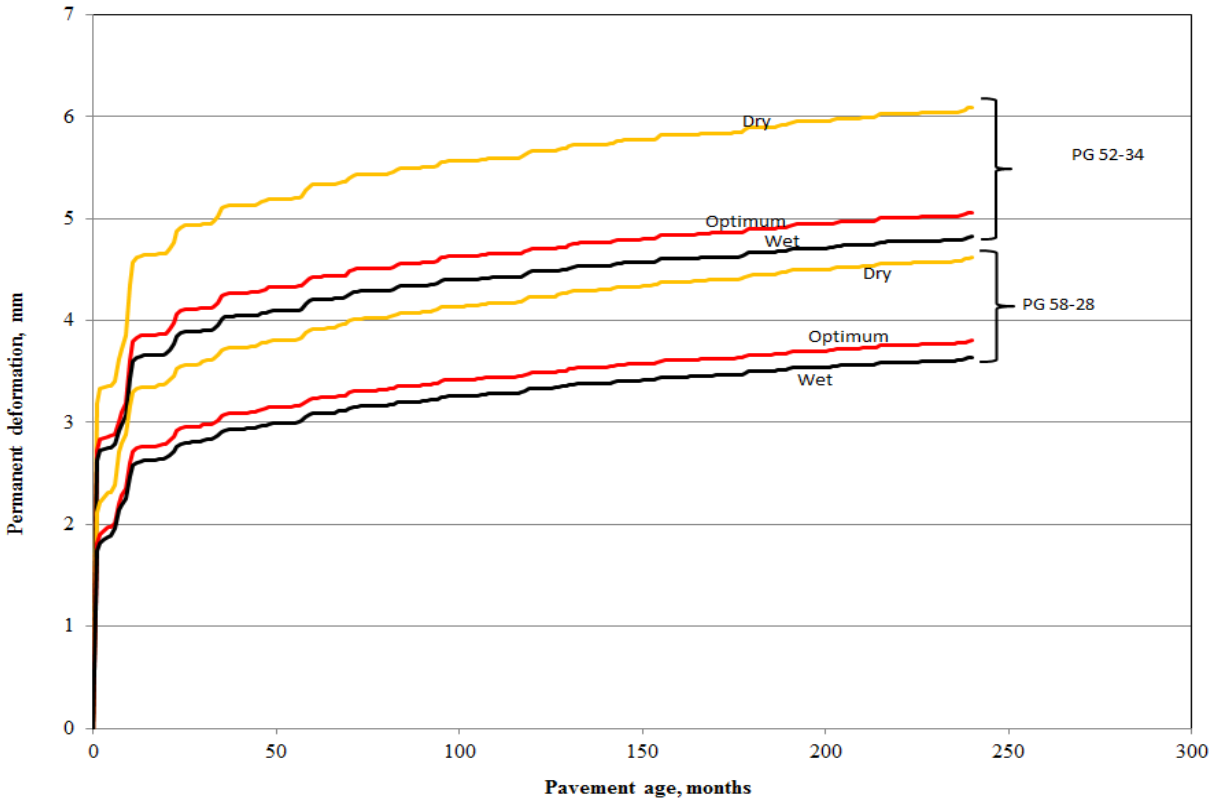

Fig 11. Permanent deformation for the granular A base material

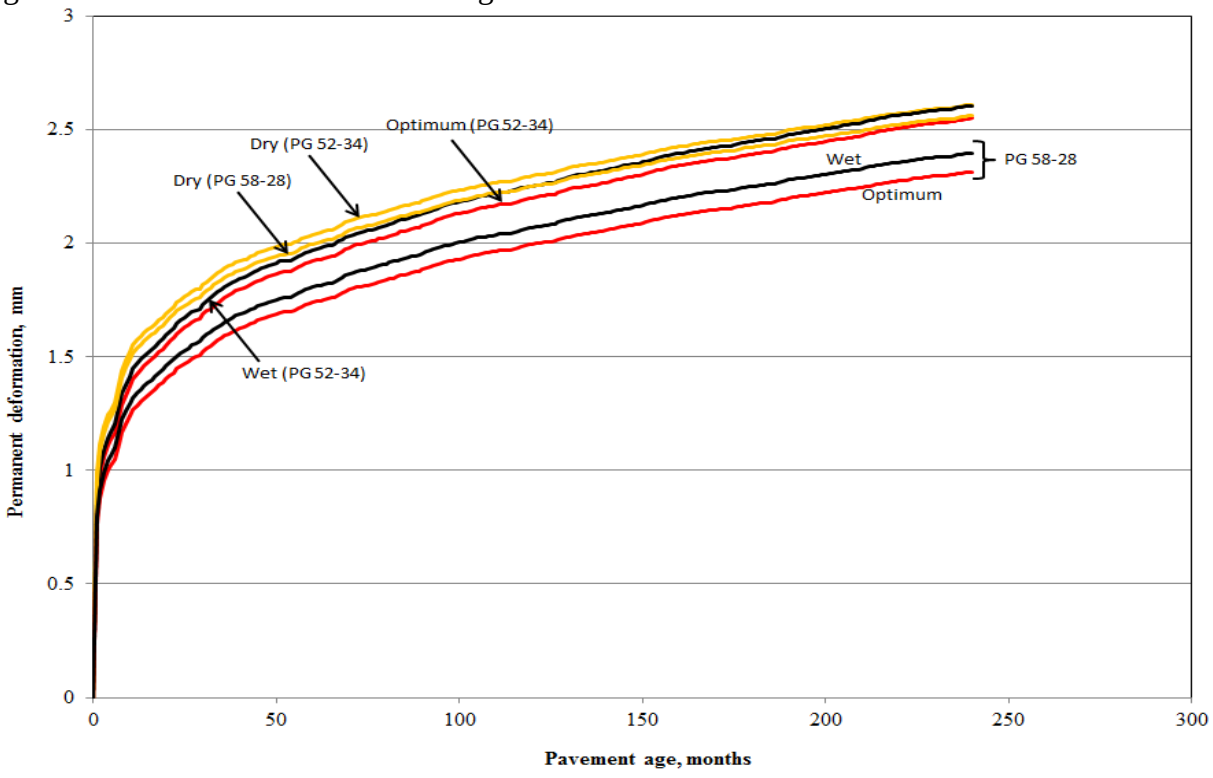

Fig 12. Permanent deformation for the Silty sand Sub-grade material